Chem. Mater. **1999,** *11,* 2305−2309

Micropatterning of Titanium Dioxide on Self-Assembled Monolayers Using a Liquid-Phase Deposition Process

K. Koumoto,* S. Seo, T. Sugiyama, and W. S. Seo

Department of Applied Chemistry, Graduate School of Engineering, Nagoya University, Nagoya 464-8603, Japan

W. J. Dressick

Naval Research Laboratory, Center for Bio/Molecular Science & Engineering (Code 6950), 4555 Overlook Ave., S.W.; Washington, D.C. 20375-5348

Received April 26, 1999
Revised Manuscript Received July 7, 1999

Biomimetic materials chemistry has recently become a very attractive field as it is expected to open new pathways for inorganic materials synthesis at low temperatures through low-energy processes.[1] Control of the crystal axis orientations and morphologies of inorganic materials through the choice of appropriate organic templating agents represents an important goal and critical theme of such research. A number of organic systems, including Langmuir monolayers, Langmuir−Blodgett (LB) films, reverse micelles, vesicles, liquid crystals, and self-assembled monolayers (SAMs), have been shown effective as templates for this purpose.[2]

Among these systems, SAMs formed through chemisorption of organosilanes of general formula $RSiX_3$ (where "R" is an organic functional group and "X" is an alkoxide or halide) to surface hydroxyl groups have long been popular as templating agents[3] due to their favorable film properties. For example, the spontaneous self-assembly of $RSiX_3$ species that occurs at hydroxylated surfaces generally yields homogeneous, robust SAMs strongly chemisorbed to the substrate. In addition, chemical and physical properties of the SAM are readily controlled through judicious choice of "R". These features have prompted the use of organosiloxane SAMs as templates for a variety of advanced applications, including fabrication of nonlinear optics multilayer assemblies,[4−7] alignment of liquid crystals[8−10] and conducting polymers,[11,12] and growth of oriented mineral structures[13−15] on surfaces.

The ability to alter the chemical reactivity of the "R" pendant groups through exposure to UV light,[16−20] electron[21] or ion[22−24] beams, or plasmas or low-energy electrons generated using proximal probes[25,26] represents an additional advantage in that it provides a means to create spatially well-defined reactivity templates in the organosiloxane SAM. Si−C bond cleavage predominates during exposure for many,[17,19,20,24] although not all,[16,18] organosiloxane SAMs studied to date, leading to formation of reactivity templates comprised of separate regions of intact pendant "R" groups and surface silanol species. Such simple templates have proven effective for the fabrication of biosensors[27−29] and microelectronic circuitry.[20]

The development of new methods for the selective deposition of refractory/ceramic materials onto surfaces is critically important to the future of microcircuit fabrication. For example, scaling of conventional metal oxide semiconductor field-effect transistor (MOSFET) structures to sizes approaching ~0.1 μm will require SiO_2 gates of ~2-nm thickness.[30] At these dimensions, leakage currents through the gate dielectric ($\kappa \sim 3.9$) will rise to unacceptable levels, compromising device reliability.[31] Definition of the MOSFET structure itself will become increasingly difficult, given the decreased photoresist transparencies at the deep UV wavelengths required for patterning at these dimensions.[32] Metal oxide film materials provide a means to attack these

* Corresponding author. E-mail: g44233a@nucc.cc.nagoya-u.ac.jp.

(1) *Biomimetic Materials Chemistry*; Mann, S., Ed.; VCH Publishers: New York, 1996, and references therein.
(2) Fendler, J. H.; Meldrum, F. C. *Adv. Mater.* **1995**, *7*, 7.
(3) Ulman, A. *An Introduction to Ultrathin Organic Films from Langmuir−Blodgett to Self-Assembly*; Academic Press: New York, 1991; Chapter 3, and references therein.
(4) Schrof, W.; Rozouvan, S.; Van Keuren, E.; Horn, D.; Schmitt, J.; Decher, G. *Adv. Mater.* **1998**, *10*, 338.
(5) Lin, W. B.; Lin, W. P.; Wong, G. K.; Marks, T. J. *J. Am. Chem. Soc.* **1996**, *118*, 8034, and references therein.
(6) Roscoe, S. B.; Kakkar, A. K.; Marks, T. J.; Malik, A.; Durbin, M. K.; Lin, W. P.; Wong, G. K.; Dutta, P. *Langmuir* **1996**, *12*, 4218.
(7) Jiang, H. W.; Kakkar, A. K.; Lebuis, A. M.; Zhou, H. T.; Wong, G. K. *J. Mater. Chem.* **1996**, *6*, 1075.
(8) Shenoy, D.; Grueneberg, K.; Naciri, J.; Shashidhar, R. *Jpn. J. Appl. Phys.- Part 2* **1998**, *37* (11A), L1326.
(9) Evans, S. D.; Allinson, H.; Boden, N.; Flynn, T. M.; Henderson, J. R. *J. Phys. Chem. B* **1997**, *101*, 2143.
(10) Ichimura, K.; Tomita, H.; Kudo, K. *Liq. Cryst.* **1996**, *20*, 171.
(11) Wu, C. G.; Chen, J. Y. *Chem. Mater.* **1997**, *9*, 399.
(12) Huang, Z.; Wang, P.-C.; MacDiarmid, A. G.; Xia, Y.; Whitesides, G. *Langmuir* **1997**, *13*, 6480.
(13) Mao, C. B.; Li, H. D.; Cui, F. Z.; Feng, Q. G.; Wang, H.; Ma, C. L. *J. Mater. Chem.* **1998**, *8*, 2795.
(14) Archibald, D. D.; Qadri, S. B.; Gaber, B. P. *Langmuir* **1996**, *12*, 538.
(15) Heywood, B. R.; Mann, S. *Adv. Mater.* **1994**, *6*, 9.
(16) Collins, R. J.; Shin, H.; DeGuire, M. R.; Heuer, A. H.; Sukenik, C. N. *Appl. Phys. Lett.* **1996**, *69*, 860.
(17) Dressick, W. J.; Dulcey, C. S.; Chen, M.-S.; Calvert, J. M. *Thin Solid Films* **1996**, *284/285*, 568.
(18) Jennane, J.; Boutros, T.; Giasson, R. *Can. J. Chem.* **1996**, *74*, 2509.
(19) Dressick, W. J.; Dulcey, C. S.; Georger, J. H.; Calvert, J. M. *Chem. Mater.* **1993**, *5*, 148.
(20) Dressick, W. J.; Calvert, J. M. *Jpn. J. Appl. Phys.* **1993**, *32*, 5829, and references therein.
(21) Mino, N.; Ozaki, S.; Ogawa, K.; Hatada, M. *Thin Solid Films* **1994**, *243*, 374.
(22) Schenkel, T.; Schneider, M.; Hattass, M.; Newman, M. W.; Barnes, A. V.; Hamza, A. V.; Schneider, D. H.; Cicero, R. L.; Chidsey, C. E. D. *J. Vac. Sci. Technol. B* **1998**, *16*, 3298.
(23) Younkin, R.; Berggren, K. K.; Johnson, K. S.; Prentiss, M.; Ralph, D. C.; Whitesides, G. M. *Appl. Phys. Lett.* **1997**, *71*, 1261.
(24) Ada, E. T.; Hanley, L.; Etchin, S.; Melngailis, J.; Dressick, W. J.; Chen, M.-S.; Calvert, J. M. *J. Vac. Sci. Technol. B* **1995**, *12*, 2189.
(25) Brandow, S. L.; Calvert, J. M.; Snow, E. S.; Campbell, P. M. *J. Vac. Sci. Technol. B* **1997**, *15*, 1455, and references therein.
(26) Sugimura, H.; Nakagiri, N. *J. Am. Chem. Soc.* **1997**, *119*, 9226.
(27) Chrisey, L. A.; O'Ferrall, C. E.; Spargo, B. J.; Dulcey, C. S.; Calvert, J. M. *Nucleic Acids Res.* **1996**, *24*, 3040.
(28) Yan, M.; Cai, S. X.; Wybourne, M. N.; Keana, J. F. W. *J. Am. Chem. Soc.* **1993**, *115*, 814.
(29) Bhatia, S.; Teixeira, J. L.; Anderson, M.; Shriver-Lake, L. C.; Calvert, J. M.; Georger, J. H.; Hickman, J. J.; Dulcey, C. S.; Schoen, P. E.; Ligler, F. S. *Anal. Biochem.* **1992**, *208*, 197.
(30) Gilmer, D. C.; Colombo, D. G.; Taylor, C. J.; Roberts, J.; Haugstad, G.; Campbell, S. A.; Kim, H.-S.; Wilk, G. D.; Gribelyuk, M. A.; Gladfelter, W. A. *Chem. Vap. Deposit.* **1998**, *4*, 1.
(31) Brar, B.; Wilk, C. D.; Seabaugh, A. C. *Appl. Phys. Lett.* **1996**, *69*, 2728.
(32) Nalamasu, O.; Baiocchi, F. A.; Taylor, G. N. In *Polymers in Microlithography*; Reichmanis, E., MacDonald, S. A., Iwayanagi, T., Eds.; ACS Symposium Series 412; American Chemical Society: Washington, DC, 1989; p 189.

10.1021/cm990223s CCC: $18.00 © 1999 American Chemical Society
Published on Web 08/12/1999

problems due to their favorable dielectric and refractory properties. In fact, refractory oxides have already been successfully demonstrated as (i) effective plasma-resistant etchmasks in top surface imaging schemes[33] designed to address patterning transparency issues and (ii) dielectrics for MOSFET gate fabrication.[34,35] The transfer of such processes to the manufacturing environment, however, will likely require development of low- temperature, selective deposition schemes utilizing "safe" solvents (e.g., water) to meet increasingly stringent environmental regulations and satisfy pressures to continually reduce manufacturing costs.

The favorable dielectric ($25 \leq \kappa \leq 30$)[30] and refractory[32,36] properties of TiO_2 have prompted a number of studies to develop methods for selective deposition of this oxide under ambient, aqueous conditions. For example, micropatterning of metal oxides using a sol–gel method has been achieved by employing SAMs in conjunction with microcontact printing techniques.[37–39] However, these sol–gel processing techniques require a posttreatment heat cure, which can damage MOSFET devices already present on the substrate, to crystallize the as-prepared amorphous film.[40–44] Sukenik and coworkers[16,45] have previously described selective deposition of TiO_2 (anatase), formed by hydrolysis of $TiCl_4$ in aqueous HCl solution at 80 °C, onto patterned organosiloxane SAMs bearing sulfonate functional groups. Films exhibited sufficiently promising electrical properties (permittivity, resistivity, and breakdown voltage) to warrant further investigation for device applications. However, the lack of a strong UV chromophore in the alkyl siloxane SAMs employed necessitated the use of high UV doses for patterning.

We report here a new patterning process for TiO_2 deposition that utilizes an aromatic phenyltrichlorosilane (PTCS) based SAM as a patterning template. The strong deep UV absorption of the phenyl chromophore renders PTCS films susceptible to patterning via Si–C bond photocleavage at lower exposure doses than those obtained for simple alkylsiloxanes (e.g., ~350 mJ/cm^2 for PTCS vs >20 J/cm^2 for octadecylsiloxane SAMs at 193 nm[20]). The method further employs a liquid-phase deposition technique[46–49] that directly deposits crystalline TiO_2 films requiring no additional postdeposition heat cure from readily handled precursors near room temperature.

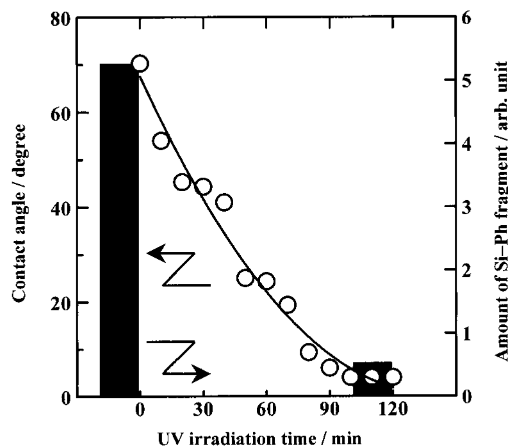

Figure 1. Curve (left scale): Water drop contact angle for PTCS SAM film as a function of UV irradiation time. Histograms (right scale): Relative quantities of phenyl functional groups remaining on the surface as a function of delivered UV dose from TOF–SIMS.

Fabrication of the patterned TiO_2 films described here involves sequential preparation and photopatterning of PTCS SAMs prior to TiO_2 deposition. Therefore, PTCS films were prepared on Si ⟨100⟩ wafers (p-type), which were first cleaned ultrasonically in deionized water (>17.6 MΩ cm), immersed in 1:1 v/v HCl/CH_3OH for 30 min, and rinsed again in deionized water. The wafers were further immersed in concentrated H_2SO_4 for 30 min and then boiling water for 5 min, and finally rinsed with acetone. The phenylsiloxane SAMs were deposited by immersion of the clean Si wafers in an anhydrous toluene solution containing 1 vol % PTCS (Aldrich Chemical Co.) for 5 min under a N_2 atmosphere. The substrates were rinsed with toluene and then baked at 120 °C for 5 min to remove residual solvent and promote SAM chemisorption.

The PTCS films were patterned by exposure to UV light (220–400 nm) from a Hg lamp through a photomask for 2 h. Cleavage of the phenyl group at the Si–C bond and subsequent formation of hydrophilic silanol groups on the surface[20] has been shown to occur as a result of 193- or 248-nm irradiation of PTCS SAMs. We verified that hydrophilic silanols were formed under flood-exposure conditions by monitoring relative concentrations of PTCS SAM phenyl groups as a function of irradiation time (Figure 1) using water drop contact angle (θ_w) and time-of-flight secondary ion mass spectroscopy (TOF–SIMS) methods. Prior to irradiation, the PTCS SAMs exhibited $\theta_w \sim 74 \pm 2°$ as expected for the homogeneous film.[20] θ_w decreased monotonically with increased UV exposure until the surface became fully wettable ($\theta_w \leq 5°$) after ~100 min. The effective level of phenyl groups in the PTCS film as measured by TOF–SIMS was decreased ~90% during this time, consistent with Si–C photocleavage and subsequent formation of hydrophilic surface silanol sites.

The generation and binding of TiO_2 (anatase) on the patterned PTCS film was effected by treatment of the irradiated SAMs with aqueous TiF_6^{2-} solutions at

(33) Eggito, F. D.; Vukanovic, V.; Taylor, G. N. In *Plasma Deposition and Etching of Polymers*; D'Agostino, R., Ed.; Academic Press: New York, 1990.
(34) Campbell, S. A.; Gilmer, D. C.; Wang, X.-C.; Hsieh, M.-T.; Kim, H.-S.; Gladfelter, W. A.; Yan, J. *IEEE Trans. Electron Devices* **1997**, *44*, 104.
(35) Kim, S.-O.; Kim, H. J. *J. Vac. Sci. Technol. B* **1994**, *12*, 3006.
(36) Katz, H. E.; Schilling, M. L.; Stein, S. M.; Houlihan, F. M.; Hutton, R. S.; Taylor, G. N. *Chem. Mater.* **1995**, *7*, 1534.
(37) Jeon, N. L.; Clem, P. G.; Nuzzo, R. G.; Payne, D. A. *J. Mater. Res.* **1995**, *10*, 2996.
(38) Clem, P. G.; Jeon, N. L.; Nuzzo, R. G.; Payne, D. A. *J. Am. Ceram. Soc.* **1997**, *80*, 2821.
(39) Xia, Y.; Whitesides, G. M. *Angew. Chem., Int. Ed. Engl.* **1998**, *37*, 550.
(40) Tohge, N.; Minami, T.; Matsuda, A.; Matsuno, Y.; Katayama, S.; Ikeda, Y. *J. Ceram. Soc. Jpn.* **1988**, *96*, 1127.
(41) Shinmou, K.: Tohge, N.; Minami, T. *Jpn. J. Appl. Phys.* **1994**, *33*, L1181.
(42) Ohishi, T.; Katoh, A. *Brit. Ceram. Trans. J.* **1993**, *92*, 79.
(43) Yogo, T.; Takeichi, Y.; Kikuta, K.; Hirano, S. *J. Am. Ceram. Soc.* **1997**, *80*, 1649.
(44) Ono, S.; Hirano, S. *J. Am. Ceram. Soc.* **1997**, *80*, 2533.
(45) Shin, H.; Collins, R. J.; DeGurie, M. R.; Heuer, A. H.; Sukenik, C. M. *J. Mater. Res.* **1995**, *10*, 692.
(46) Nagayama, H.; Honda, H.; Kawahara, H. *J. Electrochem. Soc.* **1988**, *135*, 2013.
(47) Deki, S.; Aoi, Y.; Hiroi, O.; Kajinami, K. *Chem. Lett.* **1996**, 433.
(48) Deki, S.; Aoi, Y. *J. Mater. Res.* **1998**, *13*, 883.
(49) Yao, T. *J. Mater. Res.* **1998**, *13*, 1091.

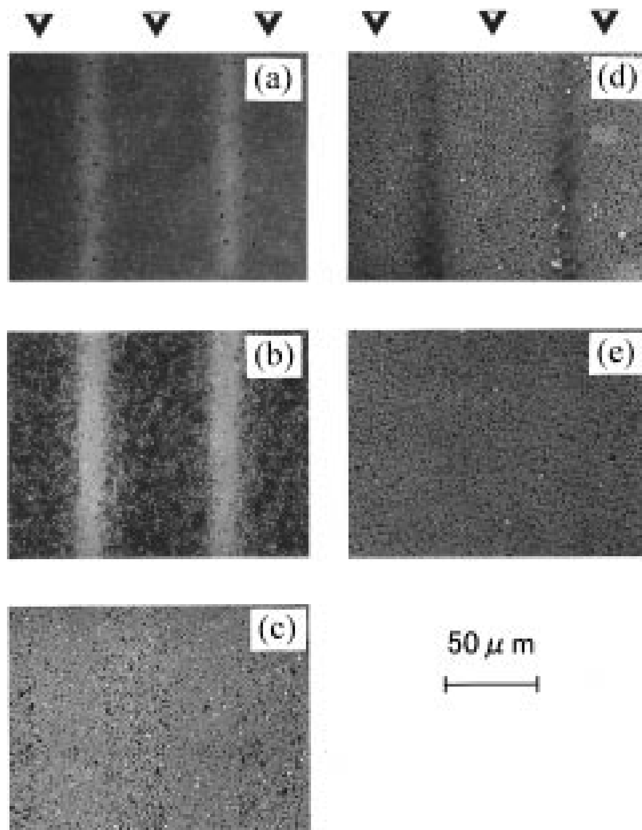

Figure 2. SEM photographs of the deposited TiO_2 films on the patterned PTCS SAM showing the morphology changes occurring with increased deposition time: (a) 2,(b) 3, (c) 4, (d) 5, and (e) 6 h. Arrows indicate position of the irradiated, hydrophilic film areas, which were readily identified from low magnification observation of the defined shape of a photomask pattern (note, e.g., Figure 4).

controlled pH. Ammonium hexafluorotitanate ($(NH_4)_2$-TiF_6 (AHFT), Mitsuwa Chemical Co.) and boric acid (H_3-BO_3, Kishida Chemical Co.) were separately dissolved in deionized water and then mixed to form a solution to which an appropriate amount of HCl was added to control the pH. Water was further added to yield a final solution containing 0.05 M AHFT and 0.15 M H_3BO_3 at pH ~2.88. The patterned PTCS SAM Si substrates were immersed in this solution at 50 °C for 12 h to deposit TiO_2. Substrates were held vertically at the bottom of this solution to prevent particles formed in the solution from accumulating on the surface. The substrate was then sonicated for 1 min, rinsed with water, and dried at room temperature.

The SEM photographs of Figure 2 show the variation of the morphology of the film deposited on the patterned PTCS SAM with deposition time. Deposition starts earlier on the intact phenyl groups of the hydrophobic surface than on the silanols of the hydrophilic surface. A large number of particles could be clearly observed on the hydrophobic surface by SEM about 90 min after initiation of the deposition reaction. The particles grow larger (Figure 2a–b) and coalesce to form a thin film (Figure 2c–e) as the deposition proceeds.

In contrast, clear evidence for deposition (i.e., particles) at the hydrophilic sites is observed only after initial formation of a very thin surface film on the substrate (compare parts a and b of Figure 2; black spots in Figure 2a indicate the presence of pores).[50] Once

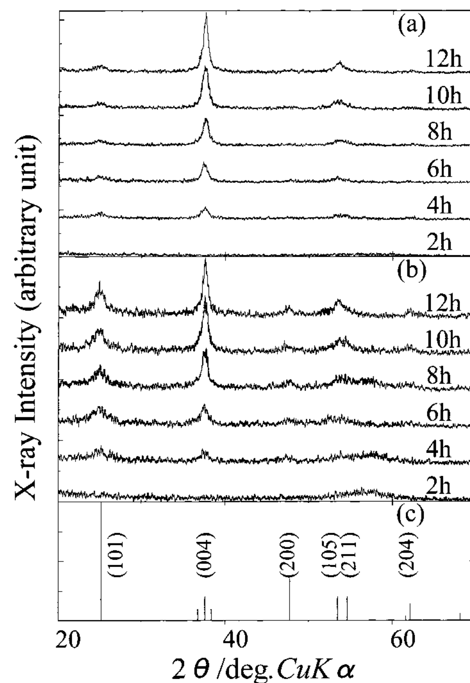

Figure 3. Variations of XRD patterns of anatase deposited with deposition time onto (a) a flood-exposed hydrophilic silanol substrate and (b) a hydrophobic phenyl substrate. Randomly oriented powder pattern for anatase (JCPDS Card no. 21-1272) (c) is shown for comparison.

formed, however, nuclei in the hydrophilic regions also promote growth and coalescence of a TiO_2 film (note Figure 2c). At longer times (Figure 2d,e), the SEM image contrast for the hydrophilic and hydrophobic regions of the PTCS SAM becomes similar as TiO_2 growth continues and the regions become almost indistinguishable.

XRD measurements in Figure 3 of the substrates following treatment with the aqueous TiF_6^{2-} solution confirm that the material deposited onto the patterned PTCS SAMs is TiO_2 (anatase) and that deposition occurs via a surface nucleation mechanism. The anatase deposited exhibits good crystallinity despite the low temperature deposition conditions. In addition, crystal planes (004) of a tetragonal unit cell are found to be highly oriented parallel to the substrate surface for anatase deposited on either the hydrophilic or hydrophobic regions of the patterned PTCS SAM, consistent with a heterogeneous surface nucleation and growth process.[51] In contrast, films formed primarily via the deposition of particles originally formed in solution are comprised of randomly oriented particulates.[51] However, although Figure 3 shows that our films are dominated by (004) oriented crystallites, small peaks due to other crystal planes such as (101) and (105) are also observed. Therefore, we cannot discount some contribution from direct deposition of particles from the solution as a parallel mechanism in the present system. Figure 3 shows that the relative intensity of (004) planes apparently increases with increasing deposition time for both hydrophilic silanol surfaces and hydrophobic phenyl

(50) X-ray photoelectron spectroscopy examination of the TiO_2 deposited on a flood-exposed (unpatterned) substrate after 1 h shows a clear $Ti(2p_{3/2})$ signal at ~458.5 eV, consistent with the presence of a TiO_2 film structure despite the absence of visible particulates in the SEM.

(51) Shin, H.; Agarwal, M.; DeGuire, M. R.; Heuer, A. H. *Acta Mater.* **1998**, *46*, 801.

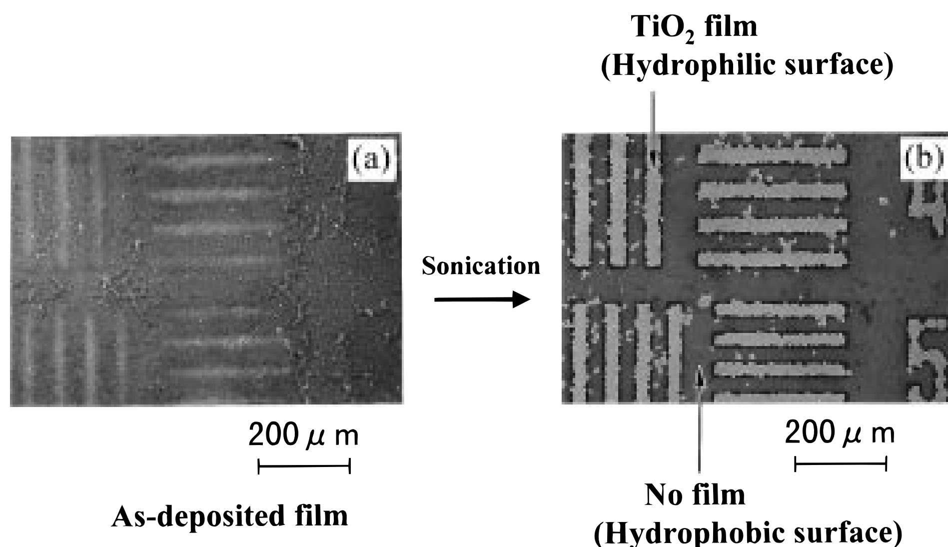

Figure 4. SEM photographs of (a) the TiO_2 film deposited on a micropatterned PTCS SAM after 6 h and (b) the micropatterned TiO_2 film remaining on the hydrophilic regions after sonication of a to remove TiO_2 present on the unirradiated, hydrophobic regions of the SAM. The PTCS SAM was first contacted with a patterned photomask and irradiated with a UV lamp to form a surface pattern, which was then treated to induce TiO_2 deposition as described in the text.

surfaces. The fraction of randomly oriented particles in the film can be estimated from the relative intensities of (004) and (101) peaks, assuming that the film was composed of both (004) plane oriented particles and nonoriented particles. The fraction decreases from ~0.23 after 4 h deposition to ~0.08 after 12 h deposition for the hydrophilic surface and from ~0.14 to ~0.03 for the hydrophobic surface. These low fractions of randomly oriented particles in the anatase films strongly support a heterogeneous surface nucleation and growth process as the principal deposition mechanism in our system.

The oriented deposition of anatase on both the hydrophilic and hydrophobic regions of the patterned PTCS SAM indicates that appropriate nucleation sites for TiO_2 deposition exist on both the phenyl- and siloxane-bearing surfaces. TiO_2 formation is initiated in solution by the hydrolysis of Ti precursors to form solvated aquo and hydroxo species,[52,53] which ultimately condense via elimination of water to form oxide particles. Literature precedents for the formation of materials containing Ti−O−Si bridges[54−56] support a binding mechanism in the hydrophilic SAM regions involving simple chemisorption of hydroxylated Ti(IV) species at silanol sites, resulting in the observed tetragonal TiO_2 lattice. Although preliminary attempts to directly study the Ti−O−Si interface using FT-IR and X-ray photoelectron spectroscopy have not been successful, Scotchtape adhesion peel test results indicate deposition of a strongly adherent TiO_2 film as expected for covalently bound material in the hydrophilic surface regions.

The nature of the TiO_2 nucleation sites in the hydrophobic film regions is less clear. Chemisorption of organosilanes bearing long alkyl "R" substituents leads to formation of close-packed, ordered SAMs having relatively few defects due to stabilization of the film structure by attractive van der Waals interactions between methylene units in adjacent "R" chains.[3] In contrast, organosilanes bearing only simple aromatic "R" lack this stabilizing interaction and chemisorb in a more random, disordered fashion, producing more loosely packed, higher defect-density SAMs.[57] Solvent-accessible, unreacted silanols remaining at such defects provide sites amenable for direct chemisorption of hydrolyzed Ti(IV) solution species as described for the hydrophilic pattern regions (vide supra). The accessible π-electron clouds of the chemisorbed phenyl groups surrounding defect sites further provide a means for possible interactions with Ti(IV) species, which are strong Lewis acids.[54] In fact, oriented adsorption of aromatic species[58,59] on TiO_2 and related surfaces is well-known in connection with photocatalytic remediation of contaminated ground/wastewater.[60] The presence of similar species, if any, in our system would require adsorption at a tetragonal symmetry site and sufficient lability of ligands trans to the π-bound phenyl ring(s) to permit further growth of TiO_2.[61] Both mechanisms are consistent with our observation of poor TiO_2 adhesion (failure of the Scotchtape adhesion test) in the hydrophobic pattern regions, as expected for a weakly bound deposit. However, our data are currently insufficient to determine which mechanism is valid.

Regardless of the exact nature of the deposition process, however, the large differences in adhesion between the hydrophobic and hydrophilic regions of the patterned PTCS SAM can be exploited to fabricate patterned TiO_2 films. Figure 4 shows SEM photographs of an as-deposited TiO_2 film (50 °C, 6 h) on a micro-

(52) Nabivanets, B. I.; Kudritskaya, L. N. *Russ. J. Inorg. Chem.* **1967**, *12*, 789.
(53) Matijevic, E.; Budnik, M.; Meites, L. *J. Colloid Interface Sci.* **1977**, *61*, 302.
(54) Cotton, F. A.; Wilkinson, G. *Advanced Inorganic Chemistry*; Interscience Publishers: New York, 1972; Chapter 25A.
(55) Brinker, C. J.; Scherer, G. W. *Sol−Gel Science*; Academic Press: New York, 1990, and references therein.
(56) Kochar, H.; Figueras, F. *J. Catal.* **1997**, *171*, 420.
(57) Durfor, C. N.; Turner, D. C.; Georger, J. H.; Peek, B. M.; Stenger, D. M. *Langmuir* **1994**, *10*, 148.
(58) Raza, H.; Wincott, P. L.; Thornton, G.; Casanova, R.; Rodriguez, A. *Surf. Sci.* **1998**, *404*, 710.
(59) Navarrete, J.; Lopez, T.; Gomez, R.; Figueras, F. *Langmuir* **1996**, *12*, 4385.
(60) Nishida, K.; Ohgaki, S. *Water Sci. Technol.* **1994**, *30*, 39.
(61) Examples of Ti(IV) complexes exhibiting these properties are known. Specifically, π-bound cyclopentadienyl complexes of Ti(IV), which function as efficient catalysts for Zeigler−Natta polymerization reactions, adopt distorted tetragonal symmetries and display enhanced lability of ligands trans to the aromatic cyclopentadienyl group.[54]

patterned PTCS SAM before (Figure 4a) and after (Figure 4b) 10 min sonication. Although the TiO_2 initially deposits over the entire substrate, sonication effectively removes the weakly bound material in the hydrophobic pattern regions. TiO_2 deposited onto the hydrophilic portions of the pattern remains strongly bonded to the substrate to define the patterned anatase region.

There are several important points worth noting concerning Figure 4. First, TiO_2 structures of ~15 μm resolution, which correspond to the smallest features on the photomask, are successfully fabricated using our method. In addition, visual inspection of Figure 4b indicates that the continuity and selectivity of the TiO_2 deposition are generally good (vide infra). However, there are clear indications of variations in feature edge roughness. For example, Figure 5 shows an SEM photograph (part a) and corresponding EDX Ti X-ray surface map (part b) of nominal 25-μm anatase line features from Figure 4b. Although the X-ray image in Figure 5b confirms selective deposition of TiO_2 on the hydrophilic regions of the patterned SAM following sonication, the anatase features exhibit significant line edge roughness. Line width measurements at 15 equally spaced points on each line in Figure 5a indicate an average printed line width of 26.3 μm. Line edge roughness, as measured by the standard deviation of the line width, is ~7.3 μm. This represents an ~28% variation (i.e., 7.3/26.3) in the nominal line width, exceeding the usual 5% variation afforded by current electronics design rules.

The origins of these phenomena are as yet undetermined but likely include contributions from at least two factors. First, no efforts have yet been made to fully optimize anatase deposition selectivity, particulate size, and related factors required to improve the fidelity of feature fabrication in Figures 4b and 5a. In addition, problems naturally arising from use of a subtractive liftoff scheme must also certainly be present, given the feature size limitations inherent in such a process. In particular, liftoff of film from substrate regions where weak binding occurs requires "tearing" of the film away from that portion remaining on the more strongly bound regions, creating an edge having a roughness characterized by the cohesive properties of the film. As feature sizes shrink, a point will eventually be reached, determined by material properties, at which edge roughness will constitute an unacceptable fraction of the feature dimension and pattern degradation will occur (vide supra). In addition, for features separated by sufficiently small dimensions, it will become increasingly difficult to overcome cohesive forces anchoring undesired "bridging" material to adjacent features. Elimination of these problems will clearly require a more comprehensive understanding of the complex factors affecting the nucleation and growth of TiO_2 particles and their deposition selectivity on the patterned organosiloxane SAM, using methods previously developed for analogous selective electroless metallization processes.[62,63] Nevertheless, the system described here provides an important first step in our goal of realizing a manufacturable process for selective metal oxide deposition under ambient, aqueous conditions.

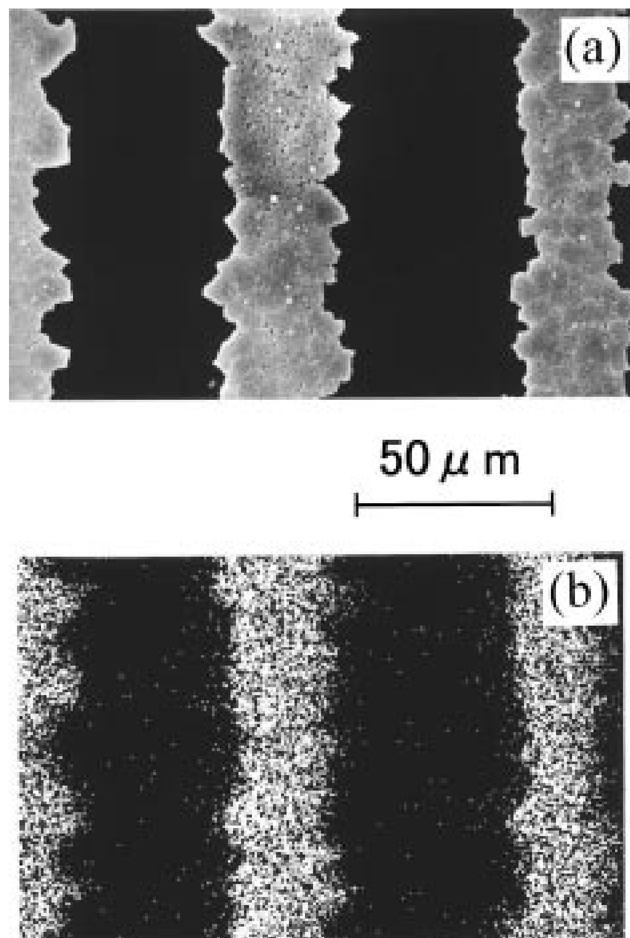

Figure 5. (a) SEM photograph of nominal 25-μm TiO_2 lines from Figure 4b, illustrating typical feature edge roughness, and (b) corresponding EDX Ti X-ray map image confirming the selective deposition of TiO_2 on the patterned surface. The light areas (hydrophilic regions) correspond to deposited TiO_2. The absence of signal (corresponding to the instrument noise level) in the dark areas (hydrophobic regions) signifies complete (i.e., >99%) removal of TiO_2 following sonication.

Acknowledgment. The authors are grateful to Dr. N. Kamiya and Mr. N. Terao of the Toyota Central R & D Labs for their assistance with TOF-SIMS, FT-IR, and XPS measurements.

CM990223S

(62) Brandow, S. L.; Chen, M.-S.; Wang, T.; Dulcey, C. S.; Calvert, J. M.; Bohland, J. F.; Calabrese, G. S.; Dressick, W. J. *J. Electrochem. Soc.* **1997**, *144*, 3425.
(63) Brandow, S. L.; Dressick, W. J.; Marrian, C. R. K.; Chow, G.-M.; Calvert, J. M. *J. Electrochem. Soc.* **1995**, *142*, 2233.